

Supplementary Information

High interstadial sea levels over the past 420ka from the Huon Peninsula, Papua New Guinea

Gino de Gelder^{1,2*}, Laurent Husson¹, Anne-Morwenn Pastier³, David Fernández-Blanco⁴, Tamara Pico⁵, Denovan Chauveau^{6,7}, Christine Authemayou⁶, Kevin Pedoja⁸

1) ISTerre, CNRS, IRD, Université Grenoble-Alpes, St. Martin d'Hères, France, 2) Res. Group of Paleoclimate & Paleoenvironment, Res. Centr. for Climate and Atmosphere, Res. Org. of Earth Sciences and Maritime, National Research and Innovation Agency, Republic of Indonesia, 3) GeoForschungsZentrum, Potsdam, Germany, 4) Barcelona Center for Subsurface Imaging, Barcelona, Spain, 5) UC Santa Cruz, Santa Cruz, USA, 6) Université de Bretagne Occidentale, Brest, France, 7) Department of Environmental Sciences, Informatics and Statistics, Ca' Foscari University of Venice, Italy, 8) Université de Caen, Caen, France

* Corresponding author: gino.de-gelder@univ-grenoble-alpes.fr

This file includes 9 Supplementary Figures, 3 Supplementary Tables and 5 Supplementary Datasets. The Supplementary Data can be retrieved with these links:

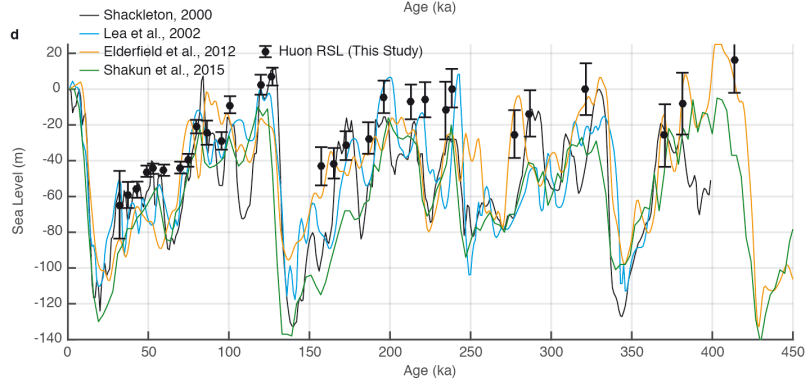
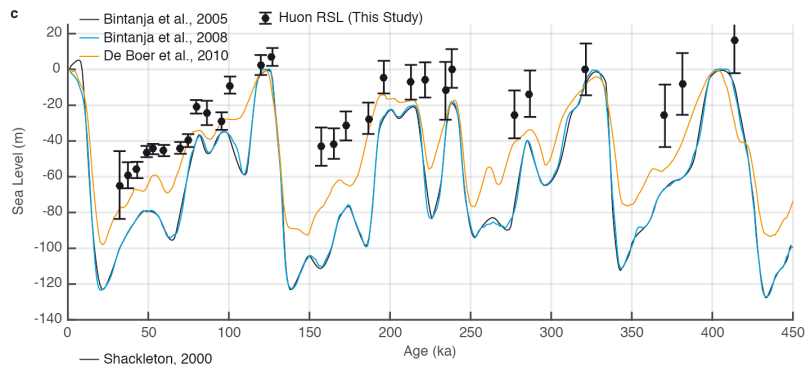
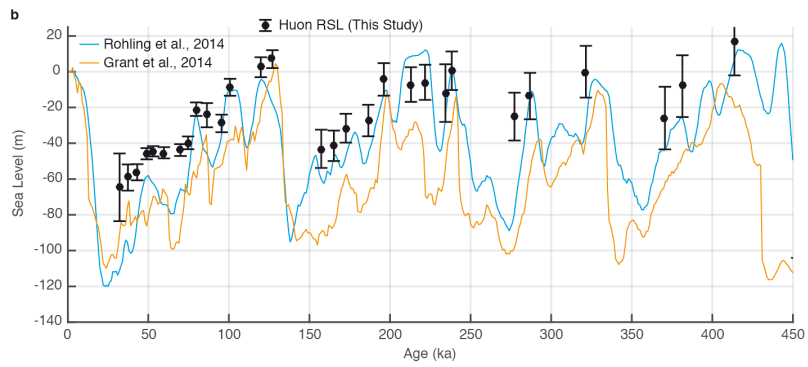
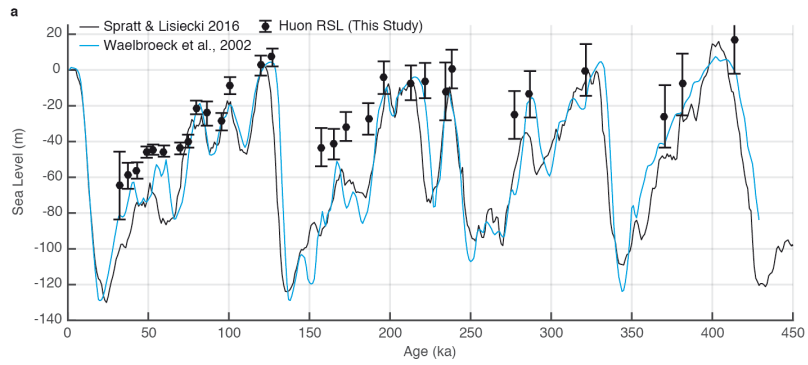
Supplementary Data 1 : <https://doi.org/10.6084/m9.figshare.15028923>

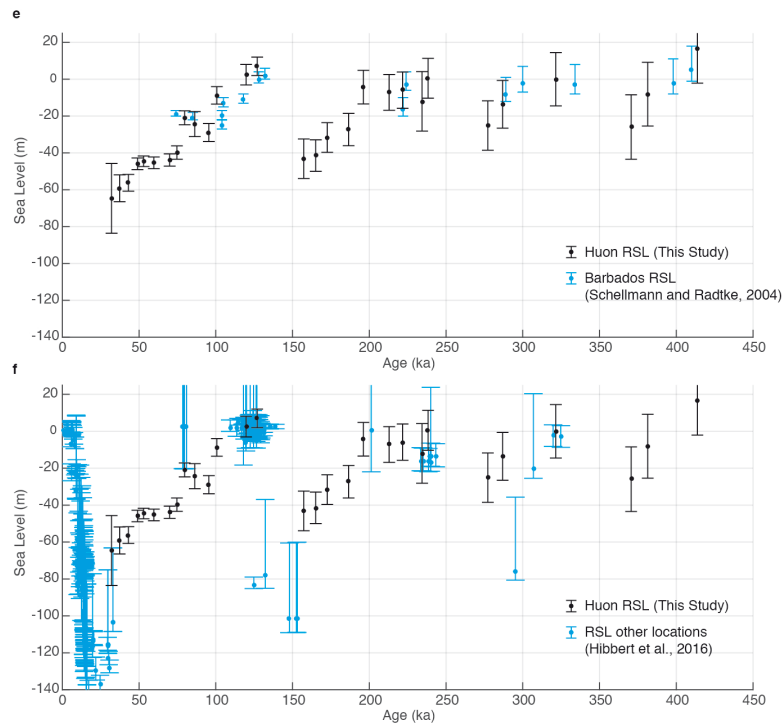
Supplementary Data 2 : <https://doi.org/10.6084/m9.figshare.20453175>

Supplementary Data 3 : <https://doi.org/10.6084/m9.figshare.15028953>

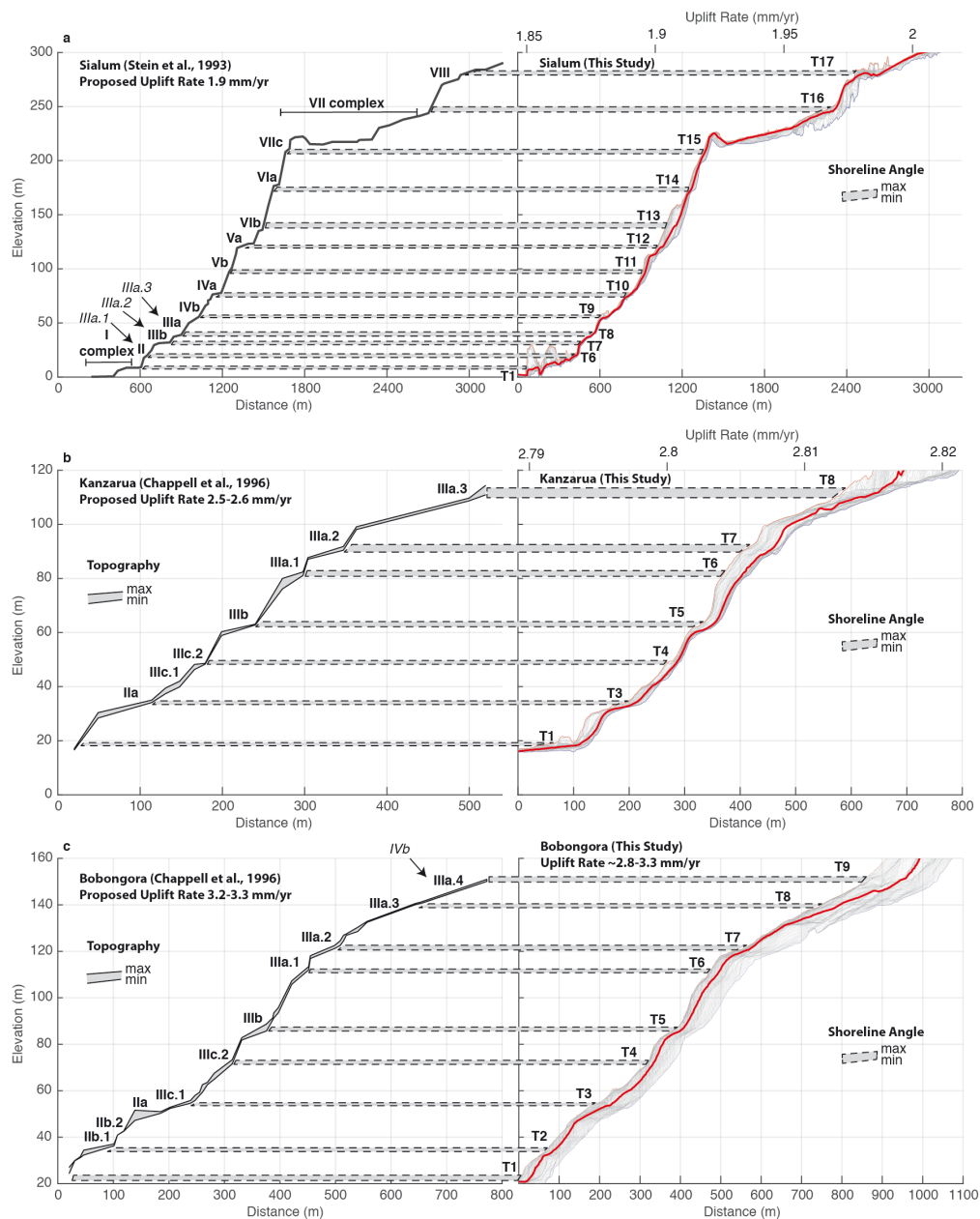
Supplementary Data 4 : <https://doi.org/10.6084/m9.figshare.15028992>

Supplementary Data 5 : <https://doi.org/10.6084/m9.figshare.21308739>

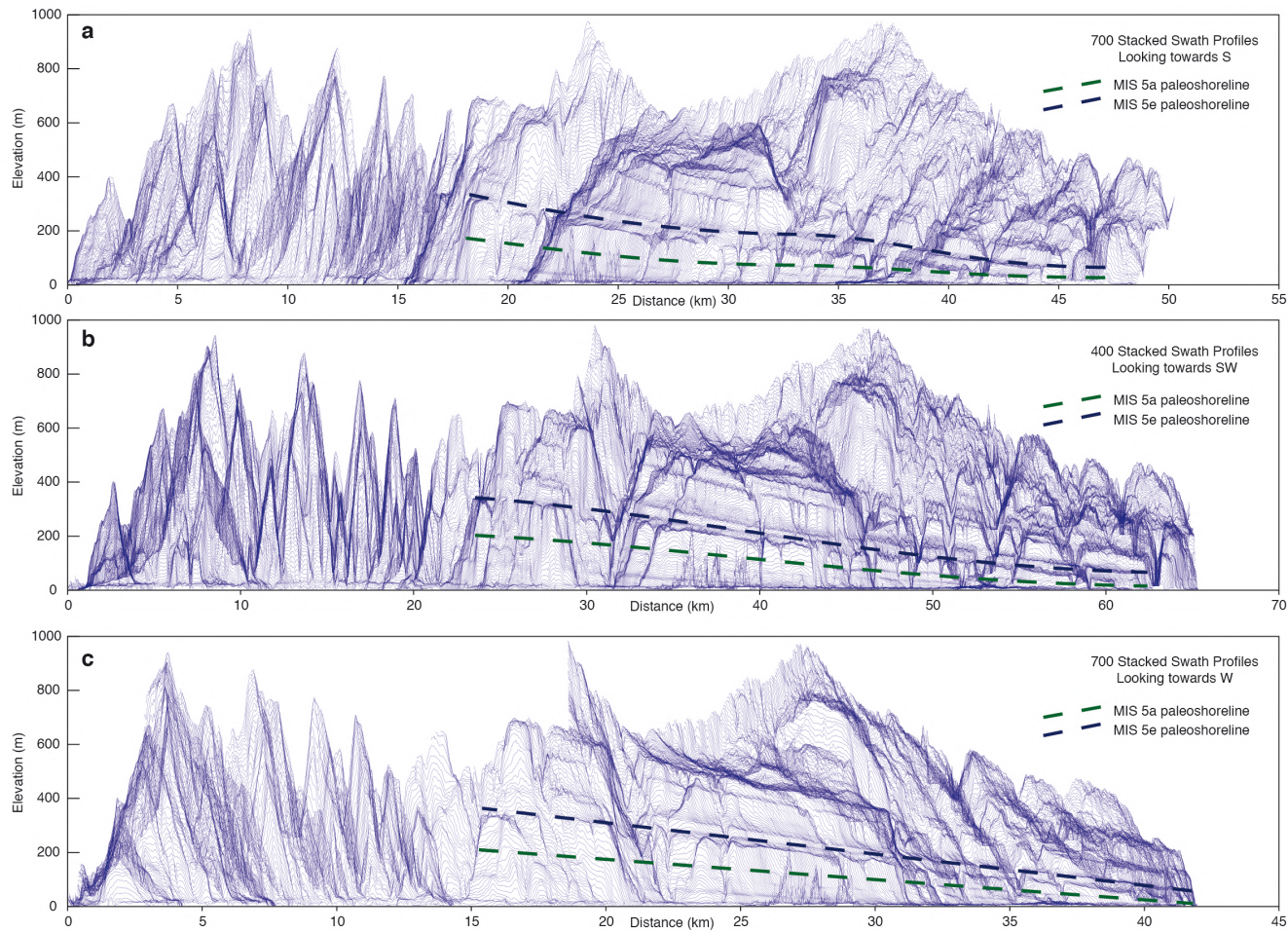




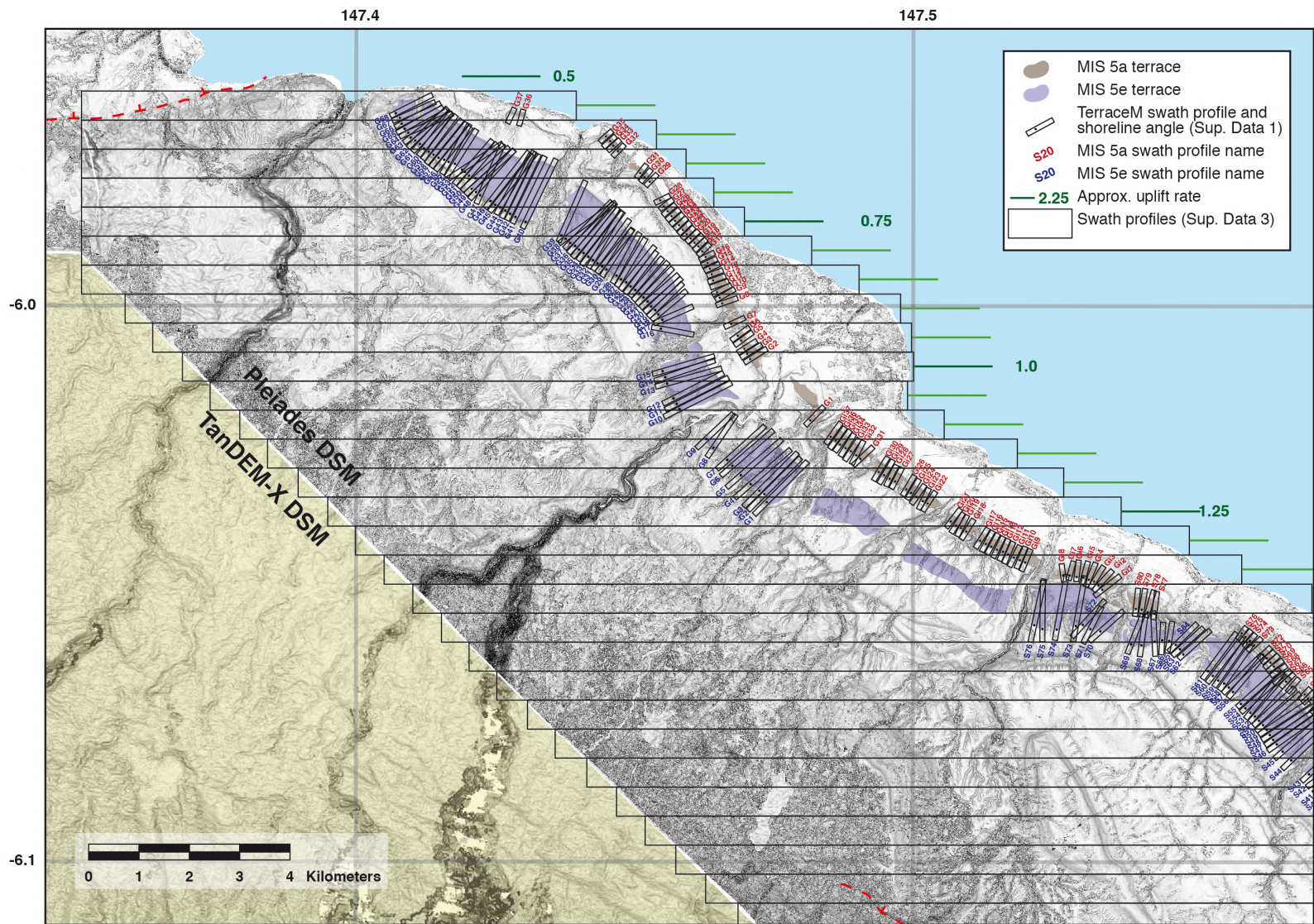
Supplementary Fig. 1: Comparison of Huon RSL with other studies. Panels **a-d** show comparison to a compilation of published sea-level curves¹, specifically with **a**) a sea-level curve calibrated with coral RSL data² and a sea-level curve derived from Principal Component Analysis³, **b**) sea-level curves derived from hydraulic control models of semi-isolated basins^{4,5}, **c**) sea-level curves derived from inverse ice volume models^{6,8} and **d**) sea-level curves in which other proxies were used to correct $\delta^{18}\text{O}$ for the temperature component⁹⁻¹². Panels **e-f** show comparisons to other locations with RSL data derived from corals and/or coral reef terraces, specifically with **e**) findings from coral reef terraces and coral ages in Barbados¹³, in which the data point represents their preferred scenario if MIS 5e was +2 m, and the upper and lower limits for scenarios with MIS 5e at +6 and 0 m respectively. **f**) Comparison of Huon RSL data with other sites around the world from a global compilation¹⁴. We left out data from Huon and Barbados, and as was done in the publication of the compilation¹⁴, we only used data with calcite <2%, ^{232}Th concentration <2 ppb, and $\delta^{234}\text{U}_{\text{total}}$ of $147 \pm 5\%$ (0-17 ka and 71-130 ka), $142 \pm 8\%$ (17-71 ka) or $147 \pm 5/-10\%$ (>130 ka). The remaining data points are from the Bahamas¹⁵, Bermuda¹⁶, Hawaii¹⁶, Curacao¹⁷, French Polynesia¹⁸⁻²⁰, Grand Cayman²¹, Mexico²², New Caledonia²³, the Pitcairn Islands²⁴⁻²⁶, the Virgin Islands²⁷, Vanuatu²⁸ and W-Australia^{24,28,29-34}. For these data points, error bars represent standard deviation 1σ . For **a-f**, error bars for Huon RSL data points indicate Standard Errors (see Methods).

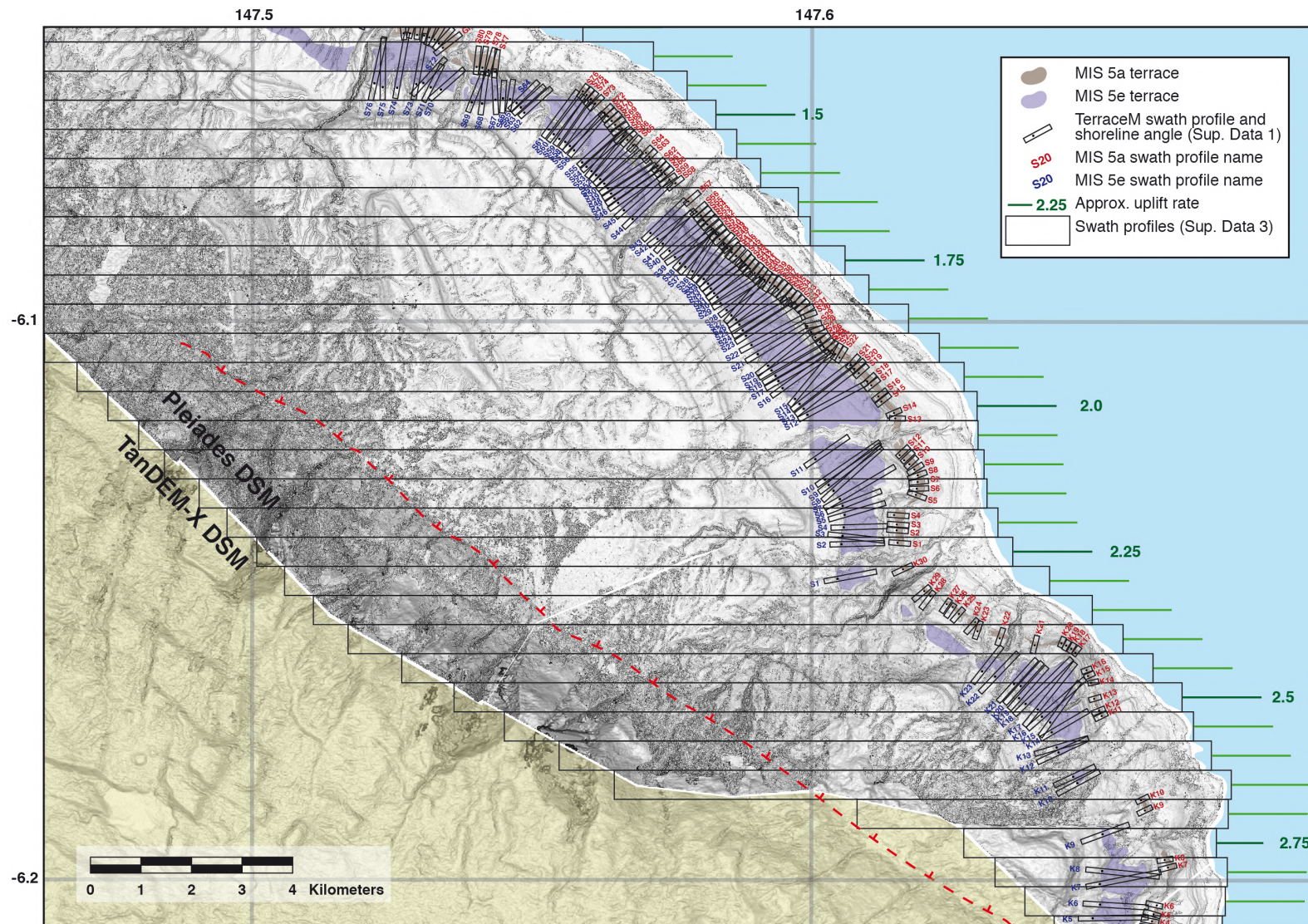


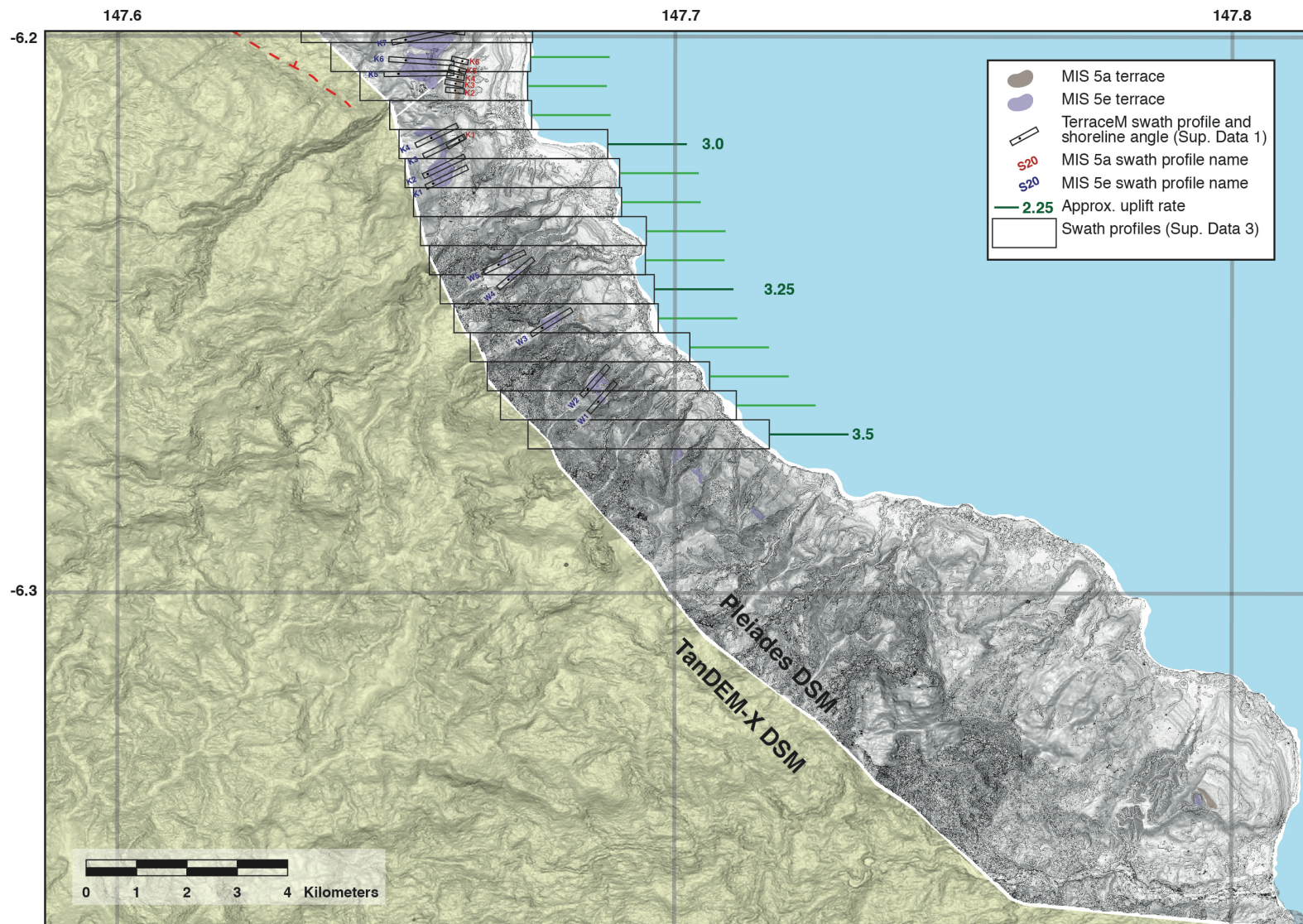
Supplementary Fig. 2. Comparison of Huon topographic profiles with previous studies. Panels on the left show profiles from **a**) Sialum³⁵, **b**) Kanzarua³⁶ and **c**) Bobongora³⁶ derived from field surveys, with the reef nomenclature as proposed in those studies. The reef names in italic indicate the revised reef name designation for the lower reefs previously (II and III), which we also use in Supplementary Table 1. The panels on the right are stacked swath profile projections³⁷ of the Pleiades Digital Surface Model (DSM), including 100 swath profiles of 2.5m width derived from a ~250m wide area around the approximate profile location of the profiles shown on the left. The median elevation is marked in red, and the dashed lines indicate the approximate terrace elevations on the Pleiades DSM. We suspect that the difference in horizontal scale in the Kanzarua and Bobongora profiles are due to measurement errors in the original publication³⁶, given that the horizontal scale of our Pleiades DSM perfectly aligns with (for example) Google Earth imagery. We do not provide precise uplift rate estimates for the Bobongora terraces, as they are discontinuously connected with the terraces at Kanzarua, Sialum and Gagar Anununai (Fig. 3), and could thus not be analysed in the same way as the other terrace profiles.



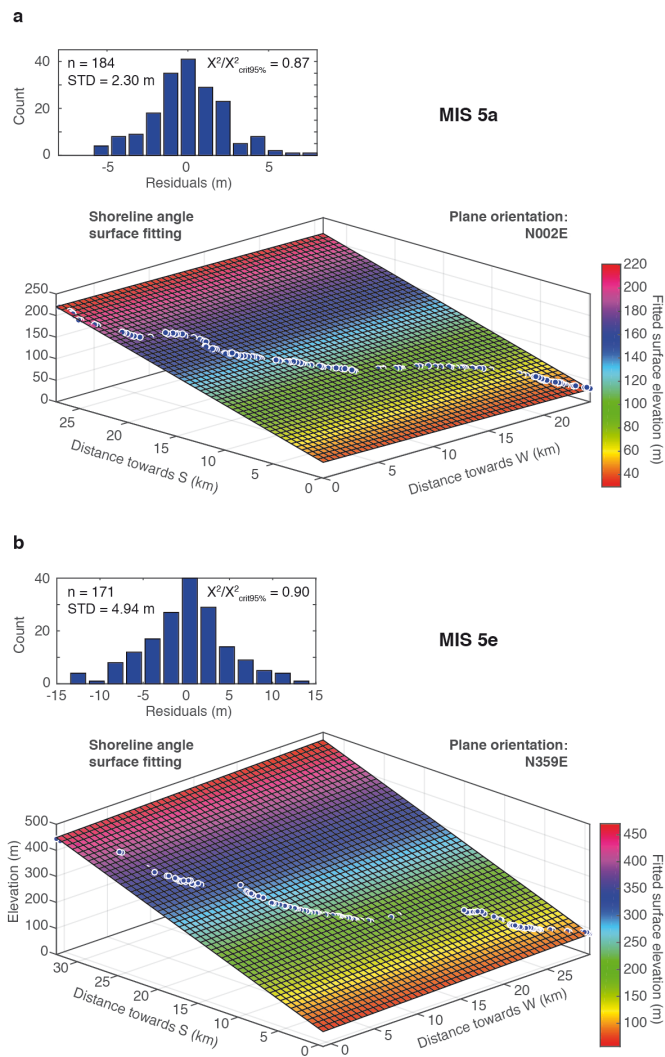
Supplementary Fig. 3: Stacked swath profile views from different directions. Stacked swath profile projections³⁷ of TanDEM-X Digital Surface Model looking towards the S (a), SW (b) and W (c), with MIS 5a and 5e paleoshorelines marked in green and blue, respectively. If the sequence is tilted, terraces would appear as straight lines when plotted across strike; the stacked swaths along different viewing directions thus suggest that the simplest approximation of the deformation pattern is a N-ward directed tilt.



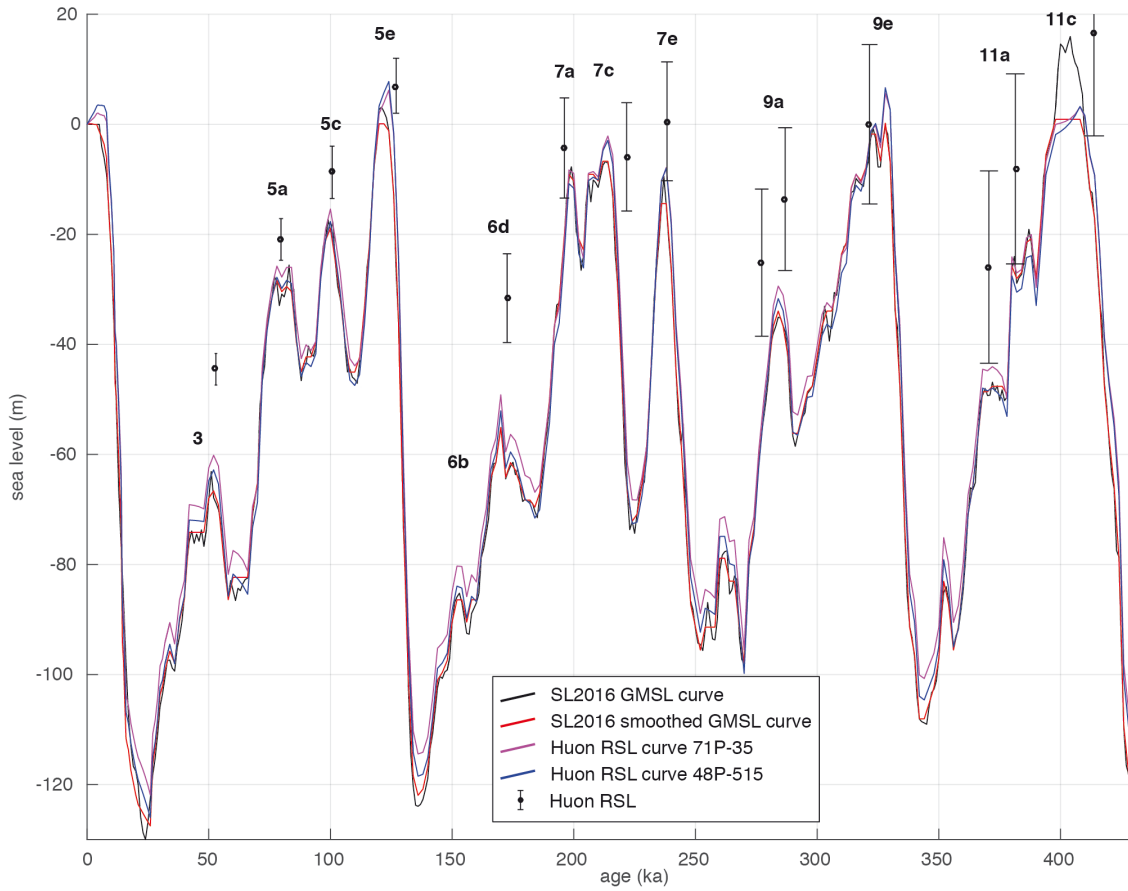




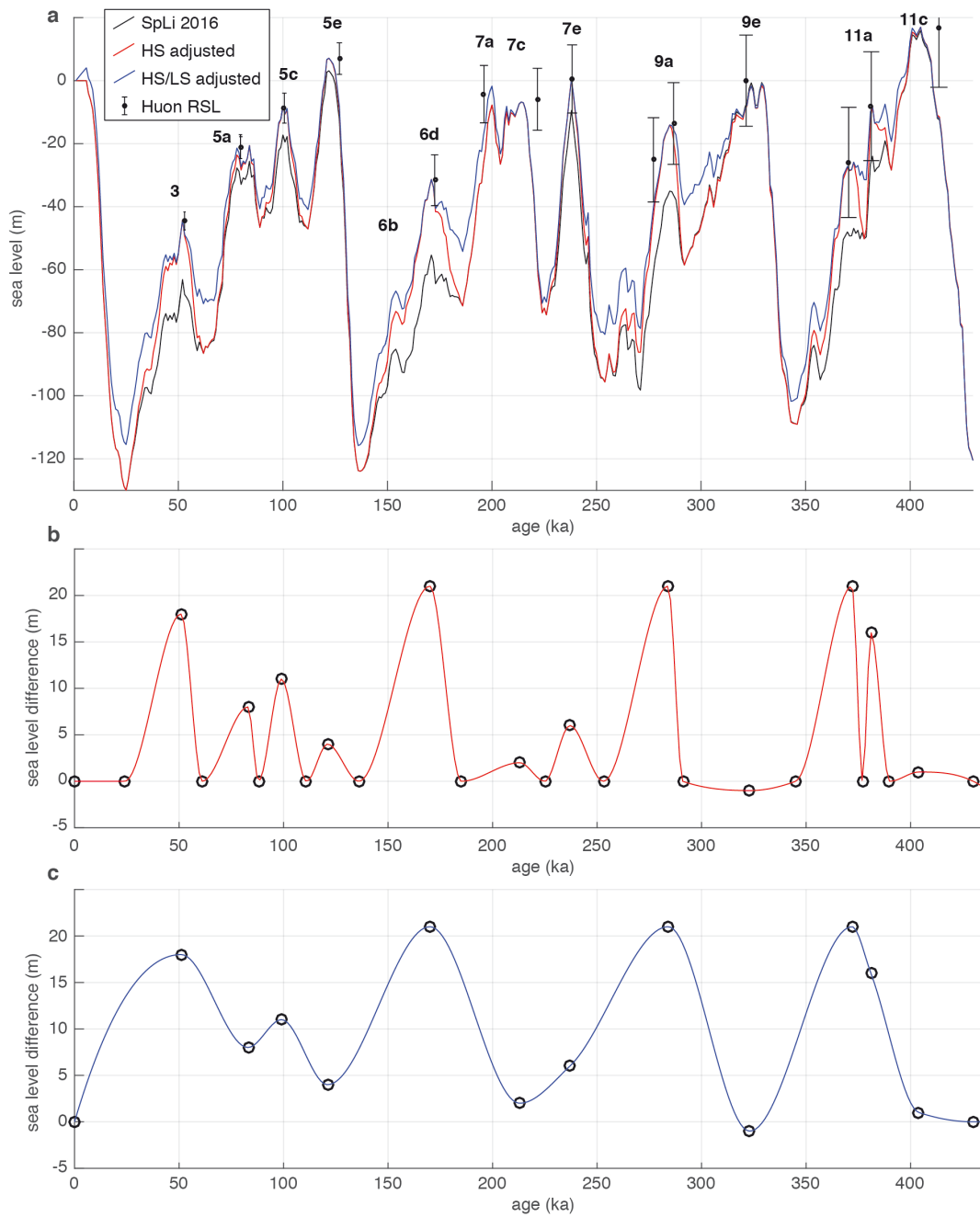
Supplementary Fig. 4: TerraceM swath profile locations. Slope maps of NW (a), central (b) and SE (c) area of the Huon coral reef terrace sequence, showing mapped MIS 5a (red) and MIS 5e (blue) terraces, as well as locations of swath profiles for TerraceM shoreline angle analysis (see methods) and large swath profiles (Supplementary Data 3). W=Wandokai, K=Kanomi, S=Sialum, Gi=Gitukia, G=Gagar Anununai. This map was made using MAPublisher version 9.8 (<https://www.avenza.com/help/mapublisher/9.8/>). Basemaps were created with Global Mapper version 15 (<https://global-mapper.software.informer.com/15.1/>).



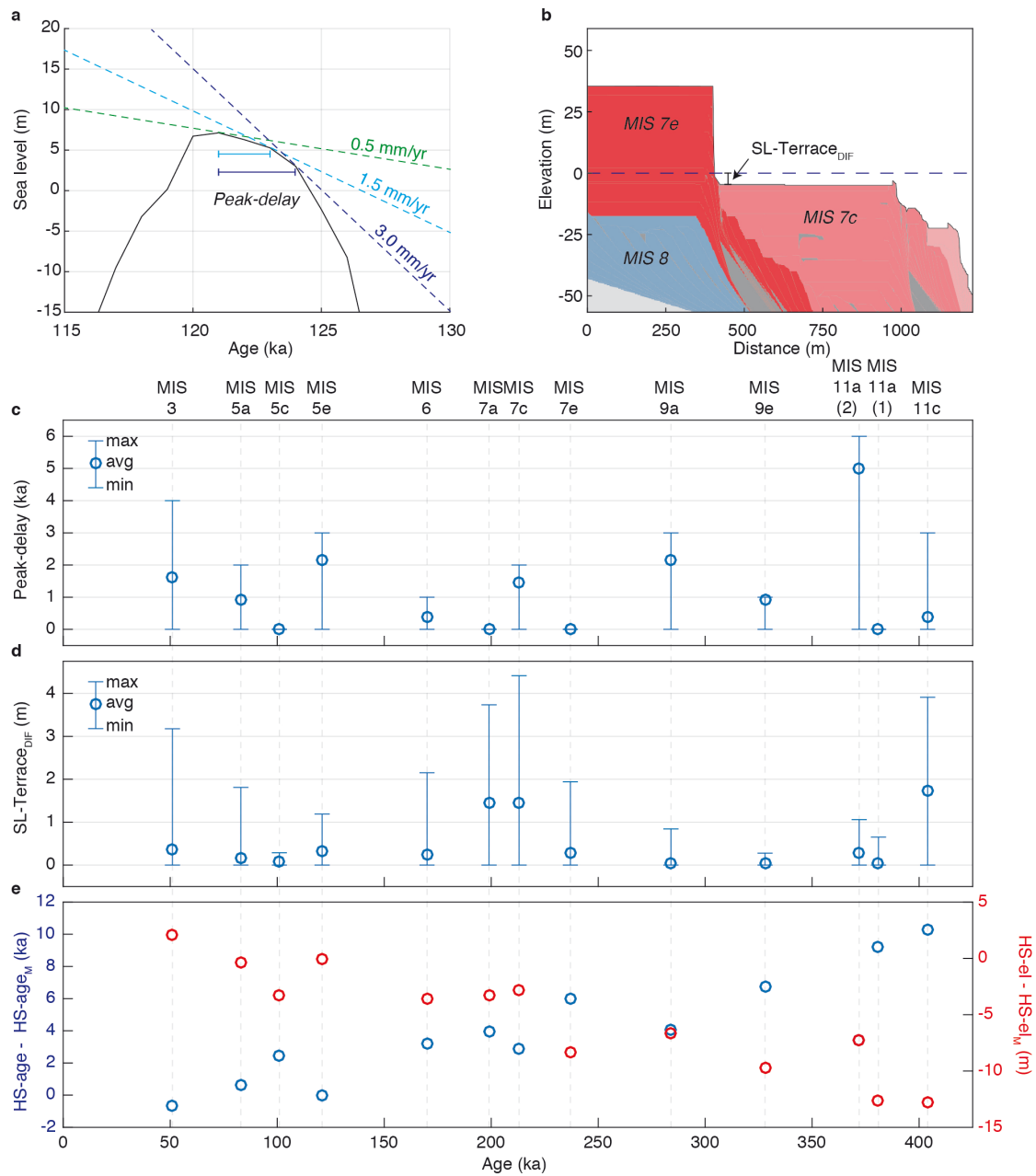
Supplementary Fig. 5: Linear surface fitting of shoreline angles. Surface fitting for **a)** MIS 5a and **b)** MIS 5e shoreline angles (same as in Fig. 2). Histogram shows residuals of surface fitting including standard deviation (STD), with distribution not significantly different from Gaussian at 95% confidence as suggested by an X^2 test.



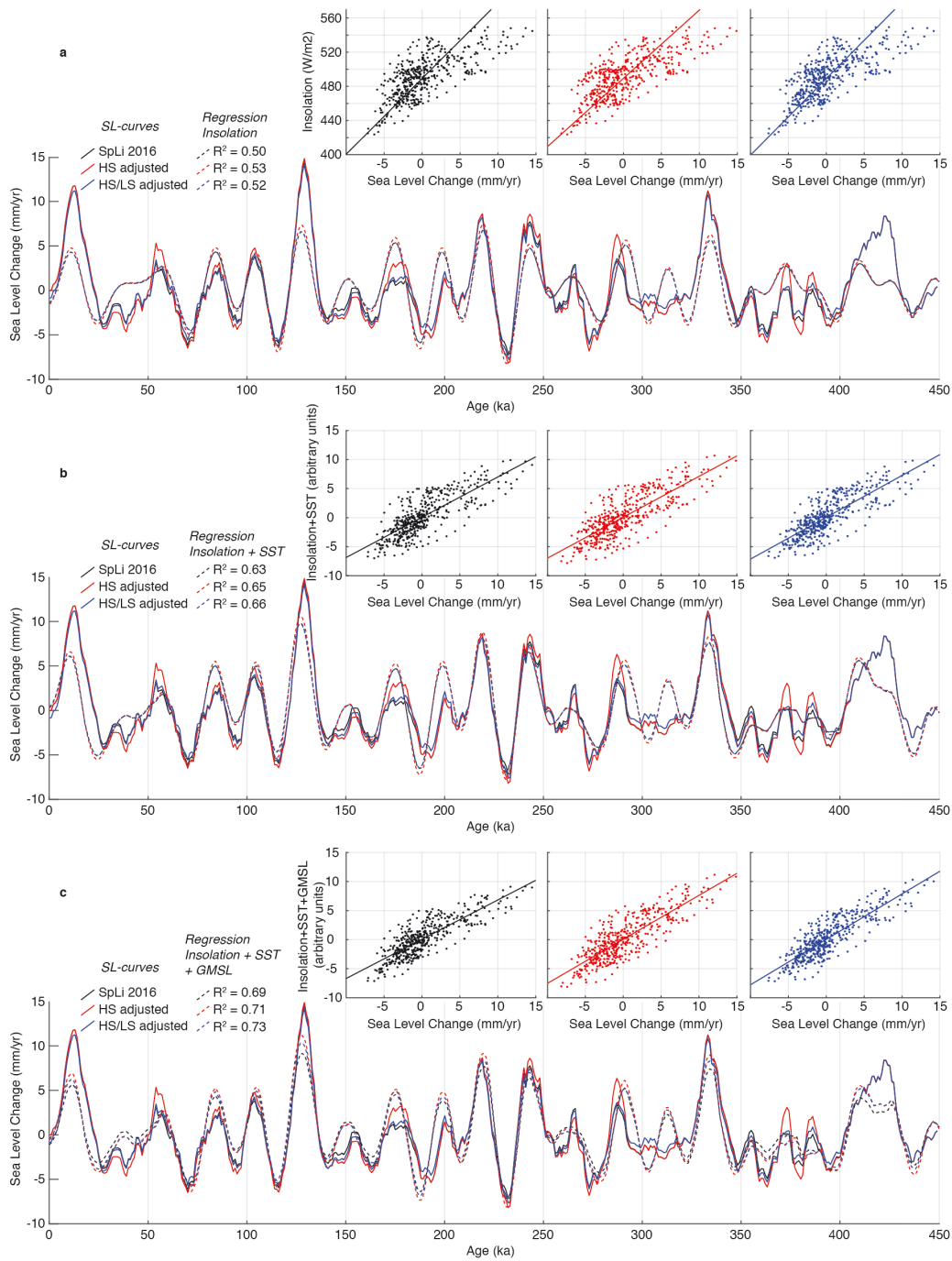
Supplementary Fig. 6: Glacio-Isostatic Adjustment corrected sea-level. Global Mean Sea Level estimates from a Principal Component Analysis³ (black), a downsampled version of that curve (red), and two Huon relative sea-level curves (purple and blue) calculated from the global ice history associated with the downsampled GMSL curve with two different earth models (see Methods). Marine Isotope Stages are labeled in bold. Error bars for Huon RSL data points indicate Standard Errors (see Methods).



Supplementary Fig. 7: Modifying SL-curves. a) Sea-level curves used for terrace modelling, including a GMSL curve calculated from Principal Component Analysis⁹ (black), a modified version of that curve with only the highstands adjusted (red) and a modified version with both high- and lowstands adjusted (blue). Marine Isotope Stages are labeled in bold. Error bars for Huon RSL data points indicate Standard Errors (see Methods) **b)** Modifications applied to the highstand-adjusted curve in **a** **c)** Modifications applied to the high- and lowstand adjusted curve in **a**.



Supplementary Fig. 8: Model tests to quantify sea-level pitfalls. **a)** Example of MIS 5e sea-level highstand (highstand adjusted curve of Supplementary Fig. 5), showing how different uplift rates can result in different ages for maximum relative sea-level elevations (peak-delay) **b)** Example of MIS 7c reef forming ~4m meters below sea-level for an uplift rate of 1.5 mm/yr (SL-Terrace_{DIF}) **c)** Minimum, average and maximum peak-delay calculated for modelled SL-highstands for a range of 0.5-3.5 mm/yr, potential reef growth rate of 10 mm/yr and basal slopes similar to Huon stacked swath profiles (Supplementary Data 2) **d)** Minimum, average and maximum SL-Terrace_{DIF} calculated with the same parameters as in **c)** and **e)** effects of peak-delay and SL-Terrace_{DIF} on highstand elevation and age estimates, using a forward modelling approach with the parameters in **c)** and inverting modelled shoreline angles following the same approach as in Fig. 2



Supplementary Fig. 9: Multivariate regression model of sea-level rate of change. Rate of change of the sea-level curves in Fig. 4a, calculated over a running 6-yr window and scaled to a multivariate regression model (as in previous work¹²) based on **a**) summer insolation⁹⁸, **b**) summer insolation and global sea-surface temperatures¹², and **c**) summer insolation, global sea-surface temperatures and sea-level curves in Fig. 4a. Insets show linear correlation between the dashed and solid lines for each sea-level curve.

Name	Age (ka)	Age Err (kyr)	RSL (m)	RSL Err (m)	MIS	Equiv. previous literature	Range dated samples (ka)
T2	32.12	5.87	-64.62	18.93	3 (7)	Reef IIb	33, 33
T3	37.35	2.38	-59.16	7.30	3 (6)	Reef IIa	35, 38, 42
T4	43.05	1.56	-56.21	4.54	3 (5)	Reef IIIc	
T5	44.13	1.03	-44.07	2.92	3 (4)	Reef IIIb	44, 45
T6	48.98	1.09	-45.88	3.15	3 (3)	Reef IIIal	55
T7	52.96	1.04	-44.52	2.86	3 (2)	Reef IIIam	51, 52
T8	59.68	1.17	-45.34	3.16	3 (1)	Reef IIIau	61
T9	69.96	1.19	-43.85	3.32	4	Reef IVb	65*, 68*, 70*, 72*
T10	74.70	1.29	-39.78	3.61	5a (3)	Reef IVa	65*, 68*, 70*, 72*
T11	79.71	1.38	-20.93	3.78	5a (2)	Reef Vb	93**, 93**
T12	86.32	2.26	-24.32	6.77	5a (1)	Reef Va	93**, 93**
T13	95.45	1.76	-28.91	4.91	5c (2)	Reef VIb	92, 99, 107, 113, 114, 118, 120***, 120***, 130, 138, 143
T14	100.69	1.77	-8.73	4.76	5c (1)	Reef VIa	90, 108, 113, 115, 120***, 120***, 126, 128, 129, 130, 130, 130, 131, 132, 133, 134,
T15	119.77	1.99	2.49	5.57	5e (2)	Reef VIIc	
T16	127	2	7	5	5e (1)	Reefs VIIa/VIIb	117, 118, 119, 137, 137
T17	157.30	3.42	-43.14	10.71	6b (2)	Reef VIII	
T18	165.15	3.03	-41.44	8.54	6b (1)	Reef VIII	
T19	172.58	2.90	-31.60	8.07	6d (2)	Reef VIII	
T20	186.52	3.17	-27.32	8.80	6d (1)	Reef IX	
T21	196.14	3.31	-4.29	9.10	7a	Reef IX	
T22	212.96	3.54	-7.16	9.70	7c (2)	Reef IX	
T23	221.74	3.63	-5.91	9.84	7c (1)	Reef IX	
T24	234.40	6.28	-11.97	16.14	7e (2)	Reef X	
T25	238.31	3.99	0.54	10.80	7e (1)	Reef X	
T26	277.24	5.19	-25.13	13.37	9a (2)		
T27	286.86	4.93	-13.59	12.97	9a (1)		
T28	321.53	5.48	0.01	14.48	9e		
T29	370.59	6.93	-25.94	17.48	11a (2)		
T30	381.42	6.78	-8.10	17.27	11a (1)		
T31	413.74	6.86	16.51	18.60	11c		

* Not specified if IVa or IVb

** Not specified if Va or Vb

*** Not specified if VIa or VIb

Supplementary Table 1: RSL Highstands Huon. MIS = Marine Isotope Stage, with substages as defined by Railsback et al. (2015). RSL = Relative Sea-Level elevations. Dated samples for Reefs II and III are taken from Chappell (2002), dated samples for the other Reefs from the compilation in Hibbert et al. (2016). VIIa and

VIIb are taken as one reef here, as VIIb appears to be the paleobarrier associated with VIIa (Esat et al., 1999). Bracketed numbers for MIS refer to the different RSL estimates within one MIS (1 for the oldest, etc.).

Location		Coral Reef Terrace			
Longitude (dec. deg.)	Latitude (dec. deg.)	UL [m]	LL [m]	IR [m]	RWL [m]
147.50	-6.00	-0.33	-0.97	0.64	-0.65
147.59	-6.07	-0.33	-0.97	0.64	-0.65
147.62	-6.10	-0.33	-0.98	0.66	-0.65
147.66	-6.15	-0.33	-0.99	0.66	-0.66
147.68	-6.18	-0.33	-0.99	0.66	-0.66
147.68	-6.21	-0.33	-0.99	0.67	-0.66
147.71	-6.25	-0.32	-0.99	0.67	-0.66
147.80	-6.31	-0.32	-1.00	0.68	-0.66
		Average			
		-0.33	-0.99	0.66	-0.66

Supplementary Table 2: Indicative range for coral reef terraces at Huon for present-day hydrodynamic conditions. Calculated for different locations along the coastal section using the indicative meaning calculator of Lorscheid and Rovere (2019). UL = Upper Limit, LL = Lower Limit, IR = Indicative Range, RWL = Reference Water Level

Previous work (Chappell, 1983; Chappell and Shackleton 1986; Lambeck and Chappell, 2001)

Name	Age (ka)	Age Err (ky)	Deposit Elev. (m)	Uplift Rate (mm/yr)	LS Elev. (m)	LS Err (m)
IIIa-base	47.5	2	91	3.3-3.5	-65	6
IVa-base	76	2	161	3.3-3.5	-65	10
Va-base	94	2	242	3.3-3.5	-56	8
VIa-base	103	3	277	3.3-3.5	-54	12
VIb-base	112.5	3	304	3.3-3.5	-61	9

Using uplift rates from this study

Name	Age (ka)	Age Err (ky)	Deposit Elev. (m)	Uplift Rate (mm/yr)	LS Elev. (m)	LS Err (m)
T5-base	46.6	2	91	3.075	-52.3	6
T9-base	72.3	2	161	3.115	-64.2	10
T12-base	90.9	2	242	3.145	-43.9	8
T13-base	98.1	3	277	3.156	-32.6	12
T14-base	110.2	3	304	3.175	-45.9	9

Supplementary Table 3: Tewai section lowstand calculation. LS = lowstand

References Supplementary Information

1. de Gelder, G. *et al.* How do sea-level curves influence modeled marine terrace sequences? *Quat. Sci. Rev.* **229**, 106132 (2020).
2. Waelbroeck, C. *et al.* Sea-level and deep water temperature changes derived from benthic foraminifera isotopic records. *Quat. Sci. Rev.* **21**, 295–305 (2002).
3. Spratt, R. M. & Lisiecki, L. E. A Late Pleistocene sea level stack. *Clim. Past* **12**, 1079 (2016).
4. Grant, K. M. *et al.* Sea-level variability over five glacial cycles. *Nat. Commun.* **5**, 5076 (2014).
5. Rohling, E. J. *et al.* Sea-level and deep-sea-temperature variability over the past 5.3 million years. *Nature* **508**, 477–482 (2014).
6. Bintanja, R., van de Wal, R. S. W. & Oerlemans, J. Modelled atmospheric temperatures and global sea levels over the past million years. *Nature* **437**, 125–128 (2005).
7. Bintanja, R. & van de Wal, R. S. W. North American ice-sheet dynamics and the onset of 100,000-year glacial cycles. *Nature* **454**, 869–872 (2008).
8. De Boer, B., Van de Wal, R., Bintanja, R., Lourens, L. J. & Tuenter, E. Cenozoic global ice-volume and temperature simulations with 1-D ice-sheet models forced by benthic ^{18}O records. *Ann. Glaciol.* **51**, 23–33 (2010).
9. Shackleton, N. J. The 100,000-year ice-Age cycle identified and found to lag temperature, carbon dioxide, and orbital eccentricity. *Science* **289**, 1897–1902 (2000).
10. Lea, D. W., Martin, P. A., Pak, D. K. & Spero, H. J. Reconstructing a 350ky history of sea level using planktonic Mg/Ca and oxygen isotope records from a Cocos Ridge core. *Quat. Sci. Rev.* **21**, 283–293 (2002).
11. Elderfield, H. *et al.* Evolution of ocean temperature and ice volume through the mid-Pleistocene climate transition. *Science* **337**, 704–709 (2012).

12. Shakun, J. D., Lea, D. W., Lisiecki, L. E. & Raymo, M. E. An 800-kyr record of global surface ocean $\delta^{18}\text{O}$ and implications for ice volume-temperature coupling. *Earth Planet. Sci. Lett.* **426**, 58–68 (2015).
13. Schellmann, G. & Radtke, U. A revised morpho- and chronostratigraphy of the Late and Middle Pleistocene coral reef terraces on Southern Barbados (West Indies). *Earth-Sci. Rev.* **64**, 157–187 (2004).
14. Hibbert, F. D. *et al.* Coral indicators of past sea-level change: A global repository of U-series dated benchmarks. *Quat. Sci. Rev.* **145**, 1–56 (2016).
15. Chen, J. H., Curran, H. A., White, B. & Wasserburg, G. J. Precise chronology of the last interglacial period: ^{234}U - ^{230}Th data from fossil coral reefs in the Bahamas. *GSA Bulletin* **103**, 82–97 (1991).
16. Muhs, D. R., Simmons, K. R. & Steinke, B. Timing and warmth of the Last Interglacial period: new U-series evidence from Hawaii and Bermuda and a new fossil compilation for North America. *Quat. Sci. Rev.* **21**, 1355–1383 (2002).
17. Muhs, D. R., Pandolfi, J. M., Simmons, K. R. & Schumann, R. R. Sea-level history of past interglacial periods from uranium-series dating of corals, Curaçao, Leeward Antilles islands. *Quat. Res.* **78**, 157–169 (2012).
18. Camoin, G. F., Ebren, P., Eisenhauer, A., Bard, E. & Faure, G. A 300 000-yr coral reef record of sea level changes, Mururoa atoll (Tuamotu archipelago, French Polynesia). *Palaeogeogr. Palaeoclimatol. Palaeoecol.* **175**, 325–341 (2001).
19. Thomas, A. L. *et al.* Penultimate deglacial sea-level timing from uranium/thorium dating of Tahitian corals. *Science* **324**, 1186–1189 (2009).
20. Deschamps, P. *et al.* Ice-sheet collapse and sea-level rise at the Bølling warming 14,600 years ago. *Nature* **483**, 559–564 (2012).
21. Blanchon, P., Jones, B. & Ford, D. C. Discovery of a submerged relic reef and shoreline off Grand Cayman: further support for an early Holocene jump in sea level. *Sediment. Geol.* **147**, 253–270 (2002).

22. Blanchon, P., Eisenhauer, A., Fietzke, J. & Liebtrau, V. Rapid sea-level rise and reef back-stepping at the close of the last interglacial highstand. *Nature* **458**, 881–884 (2009).
23. Frank, N. *et al.* Open system U-series ages of corals from a subsiding reef in New Caledonia: Implications for sea level changes, and subsidence rate. *Earth Planet. Sci. Lett.* **249**, 274–289 (2006).
24. Andersen, M. B. *et al.* The timing of sea-level high-stands during Marine Isotope Stages 7.5 and 9: Constraints from the uranium-series dating of fossil corals from Henderson Island. *Geochim. Cosmochim. Acta* **74**, 3598–3620 (2010).
25. Stirling, C. H. *et al.* Orbital forcing of the marine isotope stage 9 interglacial. *Science* **291**, 290–293 (2001).
26. Andersen, M. B. *et al.* High-precision U-series measurements of more than 500,000 year old fossil corals. *Earth Planet. Sci. Lett.* **265**, 229–245 (2008).
27. Toscano, M. A., Macintyre, I. G. & Lundberg, J. Last interglacial reef limestones, northeastern St. Croix, US Virgin Islands—evidence of tectonic tilting and subsidence since MIS 5.5. *Coral Reefs* **31**, 27–38 (2012).
28. Cutler, K. B. *et al.* Radiocarbon Calibration and Comparison to 50 Kyr BP with Paired ¹⁴C and ²³⁰Th Dating of Corals from Vanuatu and Papua New Guinea. *Radiocarbon* **46**, 1127–1160 (2004).
29. Stirling, C. H., Esat, T. M., McCulloch, M. T. & Lambeck, K. High-precision U-series dating of corals from Western Australia and implications for the timing and duration of the Last Interglacial. *Earth Planet. Sci. Lett.* **135**, 115–130 (1995).
30. Stirling, C. H., Esat, T. M., Lambeck, K. & McCulloch, M. T. Timing and duration of the Last Interglacial: evidence for a restricted interval of widespread coral reef growth. *Earth Planet. Sci. Lett.* **160**, 745–762 (1998).
31. Eisenhauer, A., Zhu, Z. R., Collins, L. B., Wyrwoll, K. H. & Eichstätter, R. The Last Interglacial sea level change: new evidence from the Abrolhos islands, West Australia. *Geol. Rundsch.* **85**, 606–614 (1996).

32. O'Leary, M. J., Hearty, P. J. & McCulloch, M. T. U-series evidence for widespread reef development in Shark Bay during the last interglacial. *Palaeogeogr. Palaeoclimatol. Palaeoecol.* **259**, 424–435 (2008).
33. Collins, L. B., Zhao, J.-X. & Freeman, H. A high-precision record of mid–late Holocene sea-level events from emergent coral pavements in the Houtman Abrolhos Islands, southwest Australia. *Quat. Int.* **145–146**, 78–85 (2006).
34. Eisenhauer, A. *et al.* Holocene sea-level determination relative to the Australian continent: U/Th (TIMS) and ¹⁴C (AMS) dating of coral cores from the Abrolhos Islands. *Earth Planet. Sci. Lett.* **114**, 529–547 (1993).
35. Stein, M. *et al.* TIMS U-series dating and stable isotopes of the last interglacial event in Papua New Guinea. *Geochim. Cosmochim. Acta* **57**, 2541–2554 (1993).
36. Chappell, J., Ota, Y. & Berryman, K. Late quaternary coseismic uplift history of Huon Peninsula, Papua New Guinea. *Quat. Sci. Rev.* **15**, 7–22 (1996).
37. Armijo, R., Lacassin, R., Coudurier-Curveur, A. & Carrizo, D. Coupled tectonic evolution of Andean orogeny and global climate. *Earth-Sci. Rev.* **143**, 1–35 (2015).
38. Laskar, J. *et al.* A long-term numerical solution for the insolation quantities of the Earth. *Astron. Astrophys. Suppl. Ser.* **428**, 261–285 (2004).